

## Supporting Information

### Supporting methods: independent measurement of $\omega$ using subpopulation-selective FCS

In order to independently test the effect of SSA on ns-FCS curves, a custom-built confocal microscope was used to detect single-molecule fluorescence in another laboratory. Here, the setup was equipped with two continuous wave lasers operating at 488 nm (Sapphire 488-20, Coherent Inc., Santa Clara, CA) and 594 nm (1677, JDSU, Milpitas, CA). The circularly polarized laser beam was focused into the sample by a water-immersion objective (Plan Apo VC 60x WI NA=1.2, Nikon, Melville, NY). Fluorescence was collected by the same objective lens and projected onto a 50  $\mu\text{m}$  confocal pinhole. A dichroic mirror (ZT488/594rpc, Chroma Technology, Bellows Falls, VT) separates fluorescence from scattered laser light. Three different filter setups were used to distribute the collected photons on the two avalanche photodiodes (SPCM AQ 14, Perkin Elmer, Waltham, MA). For donor and acceptor autocorrelation measurements, respectively, fluorescence was filtered by band pass filters (HQ532/70 or HQ650/100, Chroma Technology, Bellows Falls, VT) and split by a 50/50 beam splitter cube onto the detectors. For cross-correlation measurements the collected light was split into donor and acceptor fluorescence by a dichroic mirror (ST595, Chroma Technology, Bellows Falls, VT) first, followed by additional filtering in each channel with the aforementioned filters. A time-to-digital converter (SC-TDC-1000/04 D, Surface Concept, Mainz, Germany) tracks arrival times of photons as well as the respective detection channel. The time resolution of the TDC used in these experiments is 82.304 ps.

The measurements of the labeled polyproline peptides were performed in 50 mM sodium phosphate buffer at pH 7.5 with 0,001 % Tween 20 to minimize surface adhesion. Autocorrelation functions were measured at concentrations of about 100 pM at 140  $\mu\text{W}$  over periods of 2 h for the donor and 4 h for the acceptor. Cross-correlation data required longer measurement durations and were performed at 80  $\mu\text{W}$ . Three measurements of 15 h respectively have been performed subsequently and the histogram data have been joined.

#### Separating molecular fluorescence from background noise

To minimize background contributions to the histograms, burst selection was performed. A photon detection event was included in molecular fluorescence if at least 10 additional photons followed in a given time interval of 1 ms. Additionally, only those events with at least 20 subsequent detection events were identified as bursts. While these numbers may still seem very low, a more restricted burst selection did not show any noticeable change in the shape of the measured correlation functions, but reduced the statistics significantly. Additionally, for cross-correlation measurements only those bursts exhibiting a FRET efficiency of  $E \geq 0.1$  were chosen to exclude donor-only events that arise due to incomplete labelling.

#### Correcting for background noise

Background noise is mostly caused by the scattering of laser light and detector dark counts and is also assumed to be Poissonian. Neglecting multi-molecule events, the magnitude of  $G_{xx}(0) = R$  (for autocorrelation measurements) is caused by background noise alone. Calculated correlation functions  $G_{xx,calc}(\tau)$  have to be modified to include this noise contribution as follows:

$$G(\tau) = (1 - R) \cdot G_{calc} + R \quad (1)$$

It can be shown that  $R$  is given by the signal-to-noise ratios  $S_1$  and  $S_2$  in the individual channels by:

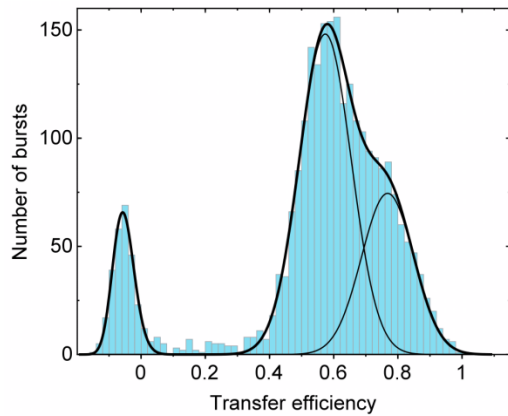
$$R = 1 - \frac{1}{\left(1 + \frac{1}{S_1}\right)\left(1 + \frac{1}{S_2}\right)} \quad (2)$$

Using the burst selection routine described before, the signal-to-noise ratio for each channel can be estimated using:

$$S_i = \frac{\left(1 - \frac{B}{T}\right)C_{B,i}}{\bar{C} - \frac{B}{T}C_{B,i}} - 1 \quad (3)$$

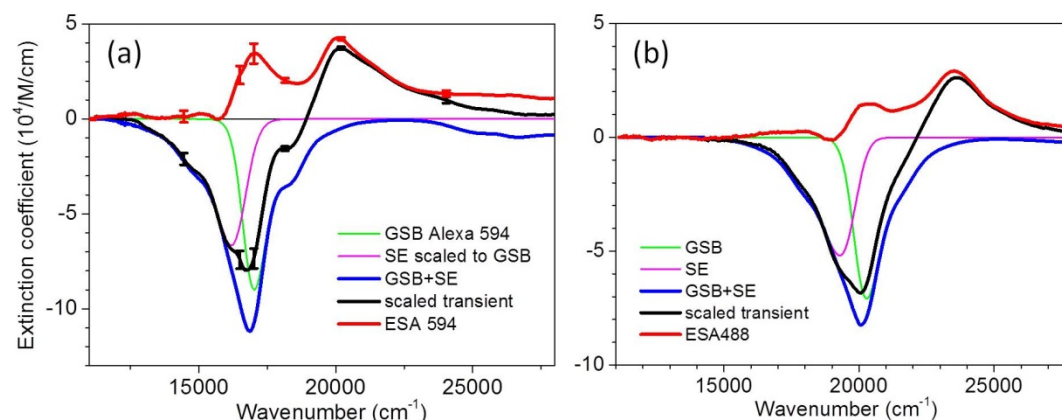
Here,  $T$  is the total measurement time,  $B$  is the accumulated burst time,  $C_{B,i}$  is the mean count rate during bursts, and  $\bar{C}$  is the overall mean count rate. While  $R$  can be determined directly for autocorrelation measurements, it has to be estimated for cross-correlation measurements using the equations above because the theoretical value for  $G_{AD}(0)$  differs from zero.

**Figure S1**



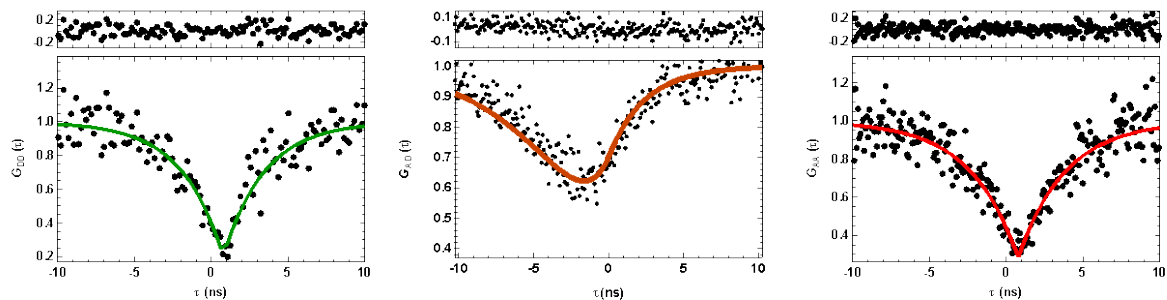
**Transfer efficiency histogram of Pro 20** (20 pM in 50 mM sodium phosphate buffer, pH 7). The larger, asymmetric peak, which corresponds to doubly labeled Pro20 is described by two Gaussian-shaped peak functions of identical width centered at  $E_1 = 0.57$  and  $E_2 = 0.77$  (thin lines). The small peak  $E \approx 0$  corresponds to a population of polypeptides lacking an active acceptor dye<sup>17</sup>. The relative populations  $c_1 = 0.59$ ,  $c_2 = 0.30$ , and  $c_{\text{only}} = 0.11$  are obtained from the three peak areas.

**Figure S2**



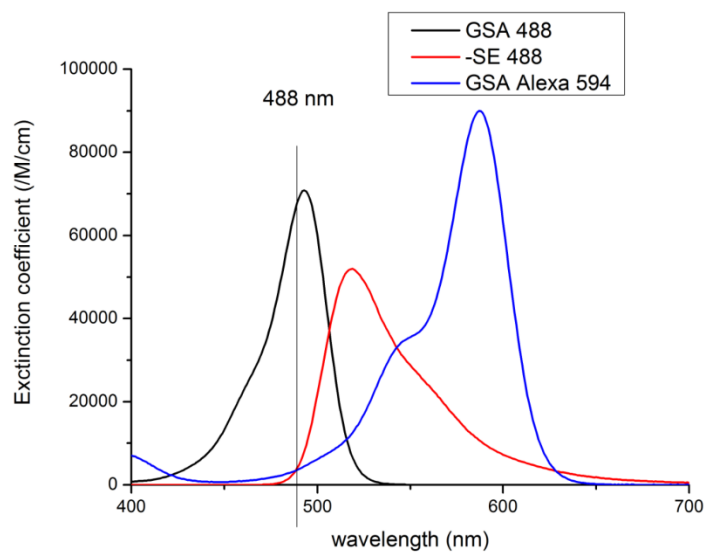
**Quantitative Determination of the Excited State Absorption Spectra of (a) Alexa 594 and (b) Alexa 488.** The black curves display the transient absorption spectra obtained for both chromophores 100 ps after impulsive excitation into S1. The green and pink curves depict the static absorption (which is used to calibrate the vertical scales) and the stimulated emission spectra computed from the steady-state fluorescence spectra (see text), respectively. The blue curve is the sum of both and should be subtracted to the scaled transient absorption signal in order to recover the ESA extinction coefficient (in red). The vanishing transient signal at energies  $< 12000 \text{ cm}^{-1}$  for Alexa 594 or  $< 15000 \text{ cm}^{-1}$  for Alexa 488, as well as the remarkable similarity between the spectral shapes of the SE and transient signal at energies  $< 16000 \text{ cm}^{-1}$  for Alexa 594 or  $< 18500 \text{ cm}^{-1}$  for Alexa 488, strongly indicate that the ESA spectra vanish in these spectral ranges. This is therefore taken as an assumption for scaling the transient spectra with respect to GSB and SE contributions, which in turn defines the accurate ESA shape. Vertical error bars in (a) are indicative of uncertainties in transient spectrum determination. This uncertainty is larger around  $16666 \text{ cm}^{-1}$ , where pump scattered light perturbs the signal. The same uncertainty holds for case (b) where pumpscattered light occurs around  $20400 \text{ cm}^{-1}$ .

Figure S3



FCS data from Pro20 labelled with AF488 as donor and AF594 as acceptor. Only selected fluorescence bursts in a 50 pM solution were subjected to correlation analysis. In the left and right panels, the donor and acceptor autocorrelation functions are plotted, and in the middle panel the acceptor-donor cross correlation function. The fit resulted in fluorescence lifetimes of 2.5 ns of the donor and 3.7 ns of the acceptor, respectively, and a  $k_{SSA}/k_T$  ratio of  $\omega=1.06\pm 0.08$ .

**Figure S4**



GSA excitation coefficients of Alexa 488 and Alexa 594 as well as the strength of SE of Alexa 488. The data allow us to quantify acceptor direct excitation (~5%) and SE (~5%) relative to the  $S_1$  excitation of Alexa 488.